

Statistical Analysis of Huge-Scale Periodic Array Antenna Including Randomly Distributed Faulty Elements

Keisuke KONNO^{†a)}, Student Member, Qiang CHEN[†], Member, Kunio SAWAYA[†], Fellow, and Toshihiro SEZAI^{††}, Member

SUMMARY On the huge-scale array antenna for SSPS (space solar power systems), the problem of faulty elements and effect of mutual coupling between array elements should be considered in practice. In this paper, the effect of faulty elements as well as mutual coupling on the performance of the huge-scale array antenna are analyzed by using the proposed IEM/LAC. The result shows that effect of faulty elements and mutual coupling on the actual gain of the huge-scale array antenna are significant.

key words: Method of Moments (MoM), impedance extension method (IEM), local admittance compensation (LAC), array antenna

1. Introduction

Recently, development of a new energy source instead of fossil fuel is an important issue to be considered for the future. Space solar power systems (SSPS) is one of the alternative energy sources and has gathered considerable attention [1], [2]. The SSPS utilizes sunlight as a power source and the energy is transmitted by using microwave from a huge-scale periodic array antenna (e.g. $10,000 \times 10,000$) on the SSPS. Therefore, analysis of the huge-scale periodic array antenna is indispensable to realize the SSPS.

For such a huge-scale array antenna, one of the interesting research topics is to investigate the effect of mutual coupling between array elements on actual gain. Since transmitting power of the array antenna is huge, accurate analysis of actual gain including the effect of mutual coupling is indispensable from a viewpoint of power efficiency. Another attractive research topic is to investigate relation between number of faulty elements and variation of actual gain. In practical operation of the SSPS, there might be some faulty elements in the power transmitting array antenna due to trouble of feeding circuits or cable disconnections. Faulty elements can cause not only reduction of mainlobe level, but also increase of sidelobe level. However, most of the researches on faulty elements in an array antenna have been limited to development of a search algorithm for faulty elements [3]–[5]. Therefore, the problem of investigating relation between number of faulty elements and variation of actual gain is still remaining as an attractive research topic

from a viewpoint of electromagnetic compatibility (EMC).

In previous researches, analysis of the periodic array antenna has been carried out by statistical or stochastic techniques. Hsiao et al. revealed that relation between errors and sidelobe level of the array antenna can be described by Nakagami-Rice distribution [6], [7]. However, relation between number of faulty elements and sidelobe level was not clearly shown in these papers. Skolnik et al. [8] proposed a technique that can design density-tapered array antenna, statistically. However, effect of mutual coupling between elements was ignored in this paper due to the limitation of computational resources.

In recent years, numerical analysis of a large scale of periodic array antenna can be carried out easily due to the progress of computers. The method of moments (MoM) combined with fast multipole method (FMM) [9] or fast fourier transform (FFT) [10] is one of the powerful techniques for numerical analysis of the periodic array antenna. In contrast of the statistical or stochastic techniques, the MoM can analyze the periodic array antenna including mutual coupling and edge effects. However, it is still impossible to analyze a huge-scale array antenna with hundreds of millions of elements by the MoM, even though powerful computers with large memories are available.

To overcome above difficulties, the impedance extension method (IEM) [11], [12] and local admittance compensation (LAC) [13] have been proposed by the present authors. By using the IEM, it is possible to include the mutual coupling and edge effects for analysis of the huge-scale periodic array antenna having hundreds of millions of elements. In addition, the array antenna including faulty elements can also be analyzed accurately by using the IEM combined with LAC (IEM/LAC). This paper is an extension version of the conference paper [13] and the proposed IEM/LAC is applied to analysis of the huge-scale array antenna including randomly distributed faulty elements. Relation between number of faulty elements and variation of actual gain on the huge-scale array antenna is exactly estimated. Moreover, accurate analysis of mainlobe and sidelobe level including effect of mutual coupling is also carried out.

This paper is organized as follows. Section 2 presents an analysis model for faulty elements. Section 3 shows the details of IEM/LAC. In Sect. 4, relative deviation of active admittance due to faulty elements and validity of the IEM/LAC are shown by numerical simulation. In Sect. 5,

Manuscript received January 31, 2011.

Manuscript revised May 23, 2011.

[†]The authors are with the Department of Electrical Communications Engineering, Graduate School of Engineering, Tohoku University, Sendai-shi, 980-8579 Japan.

^{††}The author is with Japan Aerospace Exploration Agency, Chofu Aerospace Center, Chofu-shi, 182-8522 Japan.

a) E-mail: konno@ecei.tohoku.ac.jp

DOI: 10.1587/transele.E94.C.1611

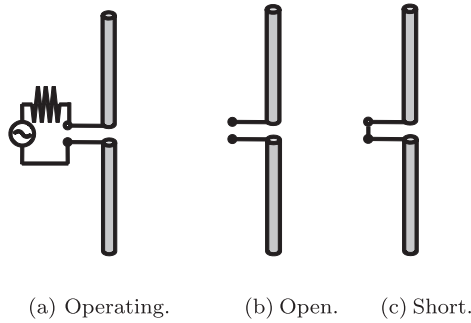


Fig. 1 Definition of faulty elements.

variation of actual gain caused by faulty elements is obtained numerically by the IEM/LAC on $10,000 \times 10,000$ array and compared with that of the Nakagami-Rice distribution, which is theoretically derived. In addition, effect of mutual coupling on actual gain is quantitatively estimated on the array antenna.

2. Analysis Model for Faulty Elements

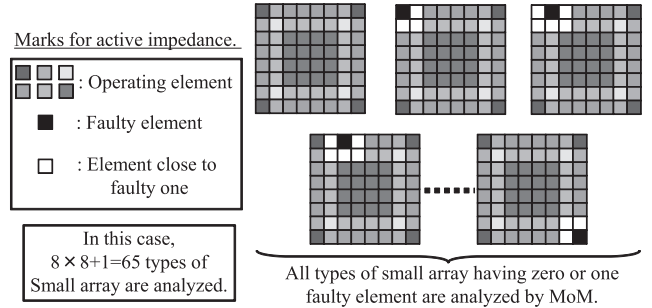
Two types of faulty elements are defined in this paper as shown in Fig. 1. Open element expresses trouble in feeding circuits due to cable disconnections, and its source resistance is set to be infinity. Short element expresses mismatching or power reduction due to damage of feeding circuits, and its source resistance and feeding voltage is set to be zero.

In practice, faulty elements shown in Fig. 1 exist randomly in a huge-scale array antenna. Faulty elements can cause active admittance variation of elements around them and also affect actual gain of the array antenna. For accurate and rapid analysis of the array antenna, the IEM/LAC, which is reviewed in next section, has been proposed [13].

3. IEM/LAC

Details of IEM/LAC are schematically shown in Fig. 2. Elements having almost same active impedance are shown by the same color in Fig. 2. As an example, 16×16 Huge array is analyzed by using active impedance/admittance of 8×8 Small array.

First, all types of Small array including one or zero faulty element are analyzed by MoM in Step 1. Next, for the Small array including one faulty element, difference of the active admittance from the Small array without faulty element is calculated and stored in Step 2. After that, the active impedance of Huge array, excepting effect of faulty elements, is obtained by using that of the Small array in Step 3. In Step 3, the active impedance of the elements in Small array is substituted into that of the corresponding elements at the corner region in the Huge array. Active impedance of the other elements in the Huge array is sequentially extended from that of the elements in the corner region as shown in Fig. 2(c). More detailed explanation of Step 3 is available in [11]. Finally, the active admittance variation of elements



(a) Step 1 Analysis for all types of Small array.

$$I_i + \Delta I_i = \frac{V_i}{Z_i + \Delta Z_i}$$

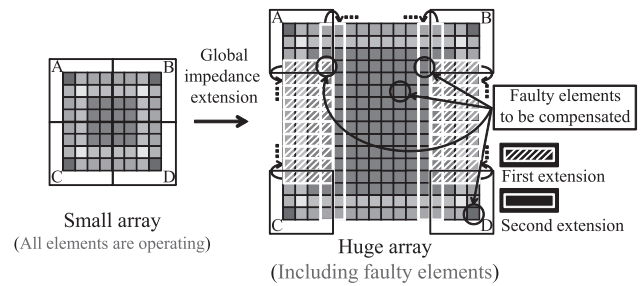
$$\Delta I_i = (Y_i + \Delta Y_i)V_i - I_i$$

$$\Delta Y_i = \frac{\Delta I_i}{V_i} \quad (i = 1, \dots, 64)$$

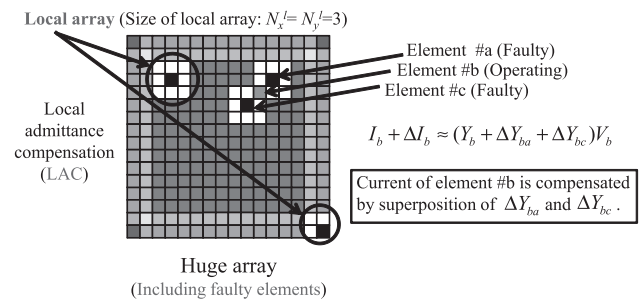
I_i, V_i : Current or voltage of feeding segment in i th element, respectively.
 Z_i, Y_i : Active impedance or admittance of feeding segment in i th element, respectively.
 Δ : Difference from small array w/o faulty elements.

This process is carried out for all small arrays.

(b) Step 2 Calculation for difference of active admittance.



(c) Step 3 Active impedance extension to Huge array.



(d) Step 4 Local admittance compensation.

Fig. 2 IEM/LAC from 8×8 Small array to 16×16 Huge array.

around faulty elements is compensated in Step 4 by using the difference obtained in Step 2, where the array having the compensated active admittance of elements is called “Local array”.

Since the LAC is based on the principle of superposition, the active admittance of elements surrounded by

some faulty elements can be compensated easily and the IEM/LAC can be applied for analysis of the Huge array including randomly distributed faulty elements.

4. Validity of IEM/LAC

In this section, validity of the IEM/LAC and optimum size of the Local array are shown based on numerical analysis. The analysis model is two dimensional cross dipole array antenna with a ground plane shown in Fig. 3. Feeding amplitude distribution for elements is 10 dB-tapered Gaussian distribution. Phase of each element is controlled for beam steering to $(\theta_{\text{main}}, \phi_{\text{main}})$. Image method is used for including effects of the ground plane. Results of all numerical analysis in this paper are obtained by supercomputing system SX-9 at Cyber Science Center in Tohoku University.

4.1 Relative Deviation of Active Admittance

First, variation of the active admittance around faulty elements is estimated by using the relative deviation defined by,

$$\Delta_Y = \frac{|Y_i^f - Y_i^o|}{|Y_i^o|} = \frac{|\Delta Y_i|}{|Y_i^o|}, \quad (1)$$

where Y_i^o is the active admittance of i th element in a Small array which does not have any faulty elements. Y_i^f is the active admittance of i th element in the Small array including one faulty element.

By using above equation, relative deviation of the active admittance is calculated and shown in Figs. 4 and 5. It is found that the active admittance variation of element around faulty one monotonically decreases as the distance between these elements increases. Therefore, the active admittance of only a few elements close to faulty one should be compensated for accurate analysis by the IEM/LAC. The optimum size of the Local array for the IEM/LAC is discussed in next numerical simulation.

4.2 Accuracy of IEM/LAC

A Huge array whose size is $N_x^h = N_y^h = 200$ is analyzed by using the conventional IEM and IEM/LAC. It is assumed

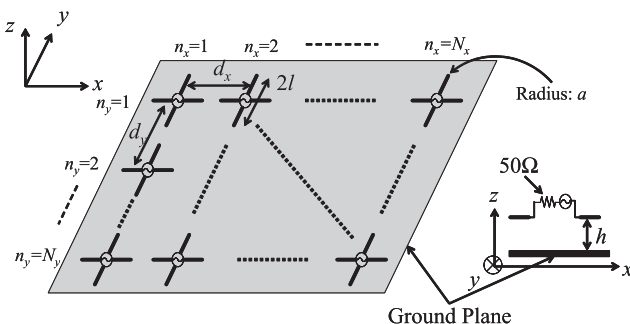


Fig. 3 Two dimensional cross dipole array antenna for SSPS.

that both open and short failures occur randomly in the same probability and P shows ratio of faulty elements in the Huge array. On the conventional IEM and IEM/LAC, the size of the Small array is $N_x^s = N_y^s = 50$. The size of Local array for the IEM/LAC is $N_x^l = N_y^l = 9$.

As an example, magnitude and phase of the active impedance of part of elements in the Huge array is shown in Fig. 6. In Fig. 6, results of “Full-wave” are obtained by MoM combined with conjugate gradient method, which is improved by parallelization and vectorization coding technique for supercomputing resources. In these figures, $n_x = 11, 14,$ and 24 are faulty elements. It is found that variation of the active impedance occurs around faulty elements. Magnitude and phase of the active impedance obtained by the IEM/LAC agrees well with that of the full-wave analysis since the LAC is carried out. CPU time required for “Full-

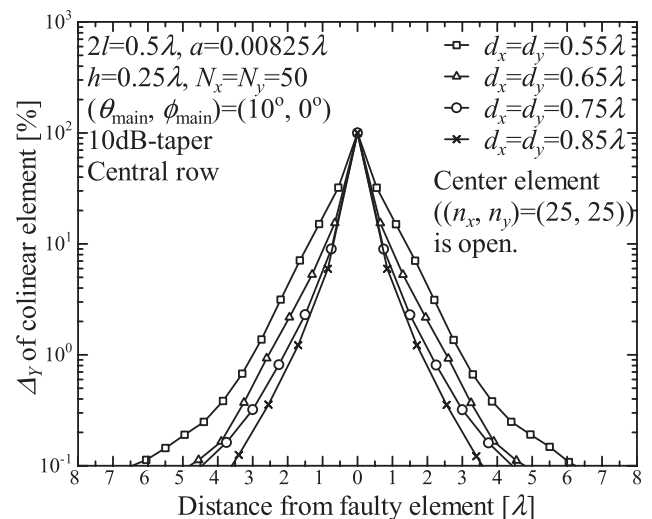


Fig. 4 Relative deviation of active admittance of elements around faulty one (open).

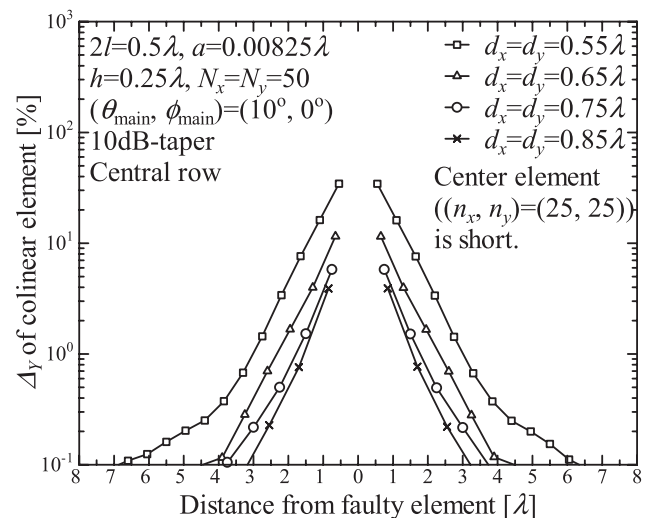


Fig. 5 Relative deviation of active admittance of elements around faulty one (short).

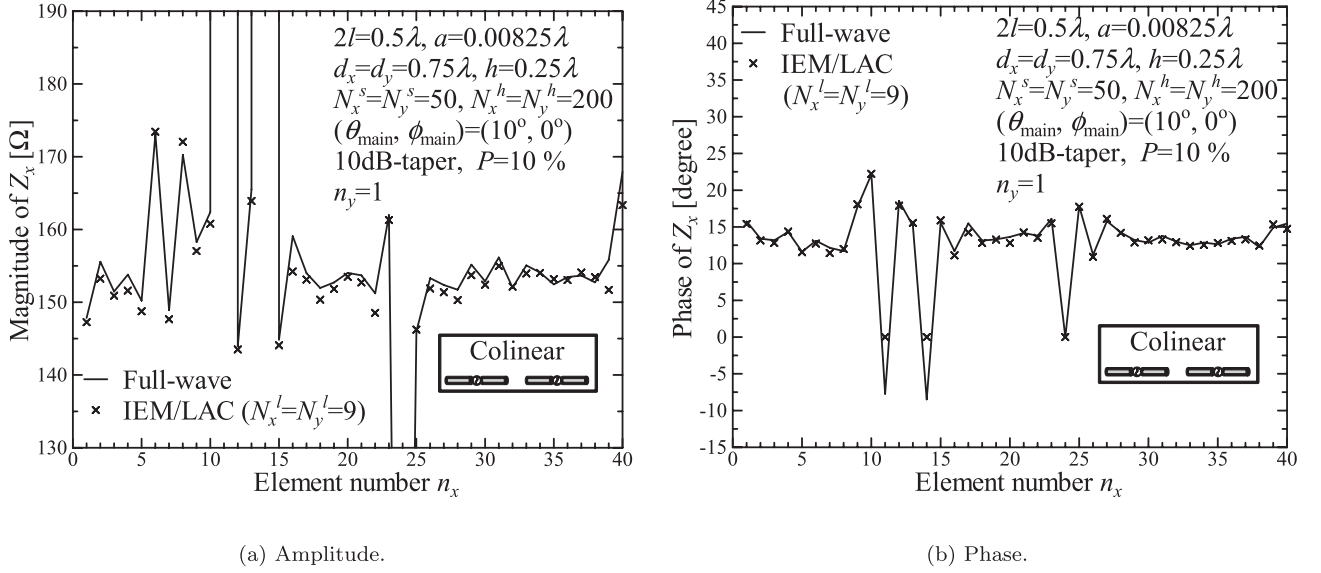


Fig. 6 Active impedance.

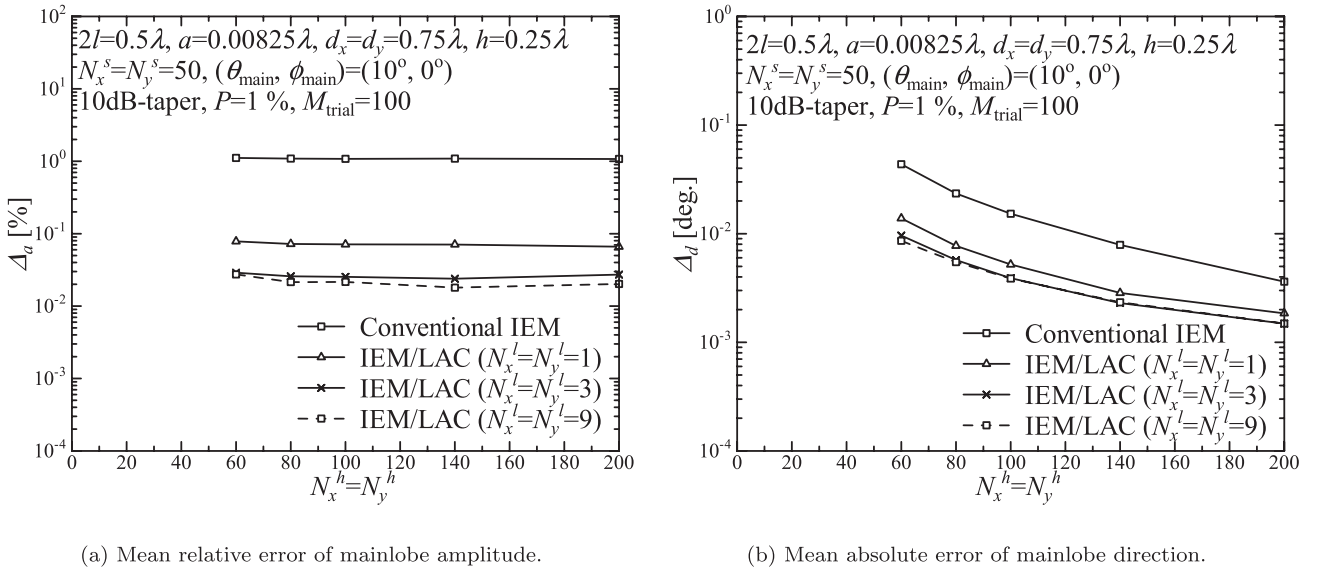


Fig. 7 Error of mainlobe.

wave” is about 7,500 sec. but that required for the IEM/LAC is only 0.1 sec., since Step 1 and 2 of the IEM/LAC had already finished before calculation.

Error for mainlobe of actual gain obtained by the IEM/LAC is calculated to estimate relation between size of Local array and error of far field. Error of amplitude and direction is estimated by following equations.

$$\Delta_a = \frac{1}{M_{\text{trial}}} \sum_{m=1}^{M_{\text{trial}}} \frac{\left| |E_m^{\text{approx}}| - |E_m^{\text{exact}}| \right|}{|E_m^{\text{exact}}|}, \quad (2)$$

$$\Delta_d = \frac{1}{M_{\text{trial}}} \sum_{m=1}^{M_{\text{trial}}} \left| \theta_m^{\text{approx}} - \theta_m^{\text{exact}} \right|, \quad (3)$$

where, $|E_m^{\text{exact}}|$, $|E_m^{\text{approx}}|$ are the amplitudes of far field ob-

tained by the full-wave analysis and IEM/LAC, respectively. θ_m^{exact} , θ_m^{approx} are the directions of far field obtained by the full-wave analysis and IEM/LAC, respectively. M_{trial} is the number of trials.

Error estimation results are shown in Fig. 7. It is found that the actual gain obtained by the conventional IEM includes large error which is proportional to number of faulty elements because the conventional IEM ignores effect of faulty elements. On the other hand, error of the actual gain obtained by the IEM/LAC is small. However, error of the actual gain obtained by the IEM/LAC does not decrease monotonically as the size of the Local array increases. It is concluded that $N_x^l = N_y^l = 3$ (i.e., $1.5\lambda \times 1.5\lambda$) is optimum size of the Local array in the case of parameters in Fig. 7.

5. Analysis of Huge-Scale Array

In this section, a Huge array whose size is $N_x^h = N_y^h = 10,000$ is analyzed by the IEM or IEM/LAC. Array parameters are the same those to the array in the previous section and feeding amplitude distribution is 10 dB-tapered Gaussian distribution. Size of Small array for the IEM and IEM/LAC is $N_x^s = N_y^s = 50$. Size of Local array for the IEM/LAC is set to be $N_x^l = N_y^l = 3$ (i.e., $1.5\lambda \times 1.5\lambda$). For comparison, numerical results ignoring mutual coupling between elements are used (without mutual coupling). It is assumed that both open and short failures occur randomly in the same probability.

5.1 Effect of Mutual Coupling on Actual Gain

Actual gain of the Huge array whose all elements are operating is analyzed by the IEM and results are shown in Table 1. As shown in Table 1, the mainlobe level shows 0.3 dB increase due to the effect of mutual coupling. On the other hand, the sidelobe level at 40° shows 1.3 dB decrease due to the effect of mutual coupling. From a viewpoint of power efficiency and EMC, the difference of the actual gain due to mutual coupling is significant and should be accurately estimated since the array is extremely huge.

5.2 Effect of Faulty Elements on Gain Variation

For statistical evaluation of relation between number of faulty elements and actual gain, ‘‘Relative gain’’ is defined by,

$$\text{Relative gain} = |\mathbf{E}_R|^2 = \frac{|\mathbf{E}(P, \theta, \phi)|^2}{|\mathbf{E}(0, \theta, \phi)|^2}, \quad (4)$$

where \mathbf{E} is far field at (θ, ϕ) direction and P is ratio of faulty elements. In previous researches on an array antenna including random errors, it has been reported that probability density function of relative amplitude level is Nakagami-Rice distribution [6], [14].

$$p(|\mathbf{E}_R|) = \frac{2|\mathbf{E}_R|}{\sigma^2} I_0 \left(\frac{2|\mathbf{E}_R| \overline{|\mathbf{E}_R|}}{\sigma^2} \right) e^{-\frac{|\mathbf{E}_R|^2 + \overline{|\mathbf{E}_R}|^2}{\sigma^2}}. \quad (5)$$

In Eq. (5), p indicates probability density function of Nakagami-Rice distribution. $\overline{|\mathbf{E}_R|}$ is average of \mathbf{E}_R and σ^2 is variance of $|\mathbf{E}_R|$. I_0 represents zeroth-order modified Bessel function of the first kind. By using P , θ , and ϕ , we can express not only average and variance of Nakagami-Rice distribution but also its relationship as follows [8],

Table 1 Effect of mutual coupling on actual gain for $10,000 \times 10,000$ array antenna.

	Actual Gain [dBi]	
	IEM	w/o mutual coupling
Mainlobe ($\theta = 10^\circ$)	82.0	81.7
Sidelobe ($\theta \approx 40^\circ$)	-3.9	-2.6

$$\overline{|\mathbf{E}_R|} = 1 - P, \quad (6)$$

$$\sigma^2 = P(1 - P) \frac{\sum_{n=1}^N |\mathbf{E}_n(\theta, \phi)|^2}{\left[\sum_{n=1}^N \mathbf{E}_n(\theta, \phi) \right]^2}, \quad (7)$$

$$\overline{|\mathbf{E}_R|^2} = \overline{|\mathbf{E}_R|}^2 + \sigma^2, \quad (8)$$

where \mathbf{E}_n is far field from n th array element and N is total number of array elements.

From Eq. (7), it is derived that variation of mainlobe and sidelobe level due to faulty elements is entirely different as follows. For mainlobe, $\left| \sum_{n=1}^N \mathbf{E}_n(\theta, \phi) \right|^2 \propto N^2$ is easily obtained since far field from all elements are superposed in phase. From the results, $\sigma^2 \approx 0$ can be derived for mainlobe since $\sum_{n=1}^N |\mathbf{E}_n(\theta, \phi)|^2 \propto N$ and $\sigma^2 = P(1 - P) \frac{N}{N^2} \approx 0$. Since variance σ^2 means spread from average (i.e., $1 - P$), $\sigma^2 \approx 0$ shows that

$$|\mathbf{E}_R|^2 \approx \overline{|\mathbf{E}_R|^2} \approx \overline{|\mathbf{E}_R|}^2 = (1 - P)^2. \quad (9)$$

On the other hand, it is thought that the relation given by Eq. (9) is not valid for a sidelobe since far field from each element has phase difference. Therefore, σ^2 for the sidelobe is not zero and $\sigma^2 \neq 0$ shows that relative gain of the sidelobe may increase due to faulty elements. Based on above discussion, it is assumed that variation of mainlobe level depends only on number of faulty elements while variation of sidelobe level depends on both number and distribution of faulty elements.

Relation between number of faulty elements and relative gain of mainlobe on the Huge array is shown in Table 2. Number of trials M_{trial} for numerical simulation by the IEM/LAC is 2,000 and CPU time for each trial is about 15 sec. by using the SX-9. From Table 2, it is found that relative gain of mainlobe obtained by the IEM/LAC is almost constant for fixed P and shows good agreement with $(1 - P)^2$. In addition, the numerical results shown in Table 2 agree the previous discussion based on a stochastic theory.

On the same Huge array, percent probability that relative gain of a sidelobe at $\theta \approx 40^\circ$ is higher than abscissa is obtained and shown in Fig. 8. From the definition of relative gain expressed by Eq. (4), relative gain which is higher/lower than 0 dB in Fig. 8 means increase/decrease of sidelobe level due to faulty elements. Even when number of faulty elements distributed in a Huge array is the same, possibility of both increase and decrease of sidelobe level can

Table 2 Relation between mainlobe level and number of faulty elements.

P	$ \mathbf{E}_R ^2$ [dB]	
	IEM/LAC	$(1 - P)^2$
0.1 %	-0.0096 ~ -0.0094	-0.0087
1 %	-0.0958 ~ -0.0952	-0.087
10 %	-0.998 ~ -0.996	-0.92

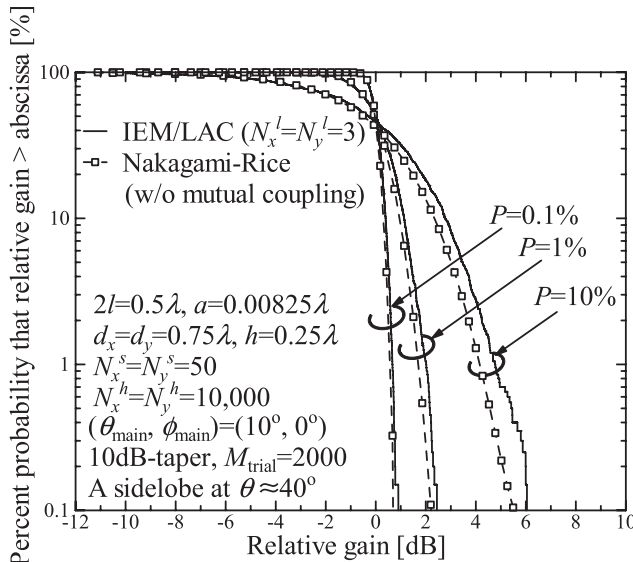


Fig. 8 Percent probability that relative gain of a sidelobe at $\theta \approx 40^\circ$ is higher than abscissa.

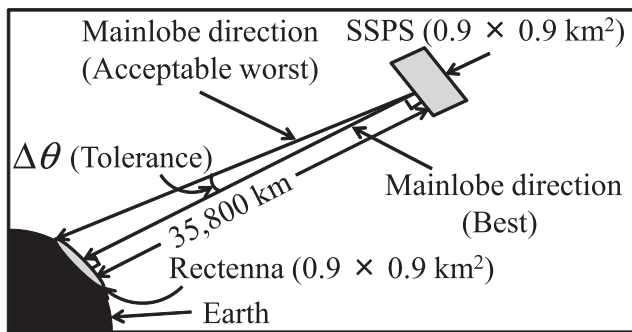


Fig. 9 Geometry of SSPS and rectenna.

occur depending on its distribution. Therefore, probability which expresses increase or decrease of the sidelobe level for fixed ratio of faulty elements P is selected as a vertical axis. From Fig. 8, it is also found that 0.4 dB (on $P = 0.1\%$), 1.1 dB (on $P = 1\%$) and 2.8 dB (on $P = 10\%$) increase of the sidelobe level can occur at 10% probability when the Huge array includes randomly distributed faulty elements. Therefore, the results show that relative gain of the sidelobe can increase due to faulty elements as previously discussed. In addition, it is also found that results obtained by the IEM/LAC show importance of mutual coupling since the increase of sidelobe level compared with the case without mutual coupling occurs. From the view of EMC, the increase of sidelobe level is critical since the array size is huge and sidelobe level is also huge.

5.3 Tolerance of Mainlobe Direction

Variation of mainlobe direction caused by faulty elements and its tolerance are the another interesting issues to be evaluated. Geometry of SSPS operating in GEO (Geostationary Earth Orbit) with rectenna is shown in Fig. 9. 2.5 GHz is

selected as operating frequency and physical size of the array antenna for the SSPS shown in Fig. 9 is obtained from the same array parameters used in this section. Size of the rectenna is assumed to be the same that of the array antenna for the SSPS.

Tolerance of mainlobe direction is defined as difference of angle between broadside and edge of the rectenna shown in Fig. 9. Therefore, tolerance of the mainlobe direction should be derived as follows.

$$\Delta\theta = \arctan\left(\frac{0.45}{35,800}\right) = 7.2 \times 10^{-4} \text{ deg.} \quad (10)$$

Numerical simulation of the error is carried out by using the IEM/LAC and number of trials $M_{\text{trial}} = 2,000$, ratio of faulty elements $P = 0.01, 0.1, 1, 10, 30\%$. As a result of our numerical simulation, maximum variation of mainlobe direction due to faulty elements is less than 10^{-7} deg. even when $P = 30\%$. This error is much less than the tolerance given by Eq. (10). Therefore, it is concluded that effect of faulty elements on the mainlobe direction can be neglected.

6. Conclusions

In this research, validity of the proposed IEM/LAC was shown and optimum size of Local array was also discussed. Based on the numerical results, optimum size of Local array was determined as $1.5\lambda \times 1.5\lambda$. By using the IEM/LAC, relation between number of faulty elements and variation of actual gain in a huge-scale periodic array antenna was also investigated. It was found that variation of mainlobe level can be estimated by only using number of faulty elements while variation of sidelobe level depends on both number and distribution of faulty elements. In addition, error of mainlobe direction due to effect of faulty elements is kept within the tolerance even when P is very large. Also, effect of mutual coupling between array elements on actual gain was quantitatively estimated. It was shown that effect of mutual coupling on the huge-scale array antenna is significant in practice due to large transmission power.

Acknowledgments

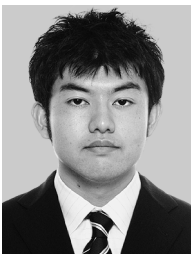
This work was supported by the GCOE Program CERIES in Tohoku University and SCAT (Support Center for Advanced Telecommunications) Technology Research, Foundation. Part of numerical results in this research was obtained using supercomputing resources at Cyberscience Center, Tohoku University.

References

- [1] P.E. Glaser, "Power from the sun: Its future," *Science*, vol.162, pp.857–861, Nov. 1968.
- [2] P.E. Glaser, "An overview of the solar power satellite option," *IEEE Trans. Microw. Theory Tech.*, vol.40, no.6, pp.1230–1238, June 1992.
- [3] O.M. Bucci, A. Capozzoli, and G. D'Elia, "Diagnosis of array faults from far-field amplitude-only data," *IEEE Trans. Antennas Propag.*,

vol.48, no.5, pp.647–652, May 2000.

- [4] A. Patnaik, B. Choudhury, P. Pradhan, R.K. Mishra, and C. Christodoulou, "An ANN application for fault finding in antenna arrays," *IEEE Trans. Antennas Propag.*, vol.55, no.3, pp.775–777, March 2007.
- [5] J.A. Rodríguez-Gonzalez, F. Ares-Pena, M. Fernandez-Delgado, R. Iglesias, and S. Barro, "Rapid method for finding faulty elements in antenna arrays using far field pattern samples," *IEEE Trans. Antennas Propag.*, vol.57, no.6, pp.1679–1683, June 2009.
- [6] J.K. Hsiao, "Normalized relationship among errors and sidelobe levels," *Radio Science*, vol.19, no.1, pp.292–302, Jan.-Feb. 1984.
- [7] J.K. Hsiao, "Design of error tolerance of a phased array," *Electron. Lett.*, vol.21, no.19, pp.834–836, Sept. 1985.
- [8] M.I. Skolnik, J.W. Sherman, III, and F.C. OGG, Jr., "Statistically designed density-tapered arrays," *IEEE Trans. Antennas Propag.*, vol.12, no.4, pp.408–417, July 1964.
- [9] K. Konno, Q. Chen, and K. Sawaya, "Quantitative evaluation for computational cost of CG-FMM on typical wiregrid models," *IEICE Trans. Commun.*, vol.E93-B, no.10, pp.2611–2618, Oct. 2010.
- [10] H. Zhai, Q. Chen, Q. Yuan, K. Sawaya, and C. Liang, "Analysis of large-scale periodic array antennas by CG-FFT combined with equivalent sub-array preconditioner," *IEICE Trans. Commun.*, vol.E89-B, no.3, pp.922–928, March 2006.
- [11] K. Konno, Q. Chen, K. Sawaya, and T. Sezai, "Analysis of huge-scale periodic array antenna for SSPS using impedance extension method," *Proc. IEICE Int. Symp. Electromagn. Compat.*, pp.33–36, Kyoto, Japan, July 2009.
- [12] K. Konno, Q. Chen, K. Sawaya, and T. Sezai, "Analysis of huge-scale periodic array antenna using impedance extension method," *IEICE Trans. Commun.*, vol.E92-B, no.12, pp.3869–3874, Dec. 2009.
- [13] K. Konno, Q. Chen, K. Sawaya, and T. Sezai, "Application of impedance extension method to 2D large-scale periodic array antenna with faulty elements," *Proc. IEICE Int. Symp. Antennas. Propag.*, vol.47, pp.1–4, Macau, China, Nov. 2010.
- [14] R.J. Mailloux, *Phased Array Antenna Handbook*, Artech House, Boston, London, 1994.



Keisuke Konno received the B.E. and M.E. degrees from Tohoku University, Sendai, Japan, in 2007 and 2009, respectively. Currently, he works for the D.E. degree at the Department of Electrical Communication Engineering in Graduate School of Engineering, Tohoku University. His research interests include computational electromagnetics, array antennas. He received the Encouragement Award for Young Researcher and Most Frequent Presentations Award in 2010 from Technical Committee on Antennas and Propagation of Japan, Young Researchers Award

in 2011 from the Institute of Electronics, Information and Communication Engineers (IEICE) of Japan.



Qiang Chen received the B.E. degree from Xidian University, Xi'an, China, in 1986, the M.E. and D.E. degrees from Tohoku University, Sendai, Japan, in 1991 and 1994, respectively. He is currently an Associate Professor with the Department of Electrical Communications, Tohoku University. His primary research interests include computational electromagnetics, array antennas, and antenna measurement. Dr. Chen received the Young Scientists Award in 1993, the Best Paper Award in 2008 from the Institute of Electronics, Information and Communication Engineers (IEICE) of Japan. Dr. Chen is a member of the IEEE. He has served as the Secretary and Treasurer of IEEE Antennas and Propagation Society Japan Chapter in 1998, the Secretary of Technical Committee on Electromagnetic Compatibility of IEICE from 2004 to 2006, the Secretary of Technical Committee on Antennas and Propagation of IEICE from 2007 to 2009. He is now Associate Editor of IEICE Transactions on Communications.

of Japan. Dr. Chen is a member of the IEEE. He has served as the Secretary and Treasurer of IEEE Antennas and Propagation Society Japan Chapter in 1998, the Secretary of Technical Committee on Electromagnetic Compatibility of IEICE from 2004 to 2006, the Secretary of Technical Committee on Antennas and Propagation of IEICE from 2007 to 2009. He is now Associate Editor of IEICE Transactions on Communications.



Kunio Sawaya received the B.E., M.E. and D.E. degrees from Tohoku University, Sendai, Japan, in 1971, 1973 and 1976, respectively. He is presently a Professor in the Department of Electrical and Communication Engineering at the Tohoku University. His areas of interests are antennas in plasma, antennas for mobile communications, theory of scattering and diffraction, antennas for plasma heating, and array antennas. He received the Young Scientists Award in 1981, the Paper Award in 1988, Communications Society Excellent Paper Award in 2006, and Zen-ichi Kiyasu Award in 2009 all from the Institute of Electronics, Information and Communication Engineers (IEICE). He served as the Chairperson of the Technical Group of Antennas and Propagation of IEICE from 2001 to 2003, the Chairperson of the Organizing and Steering Committees of 2004 International Symposium on Antennas and Propagation (ISAP'04) and the President of the Communications Society of IEICE from 2009 to 2010. Dr. Sawaya is a senior member of the IEEE, and a member of the Institute of Image Information and Television Engineers of Japan.

Dr. Sawaya is a senior member of the IEEE, and a member of the Institute of Image Information and Television Engineers of Japan.



Toshihiro Sezai received the M.E. degree from Tokoku University, Sendai, Japan, in 1988. Currently, he works in Japan Aerospace Exploration Agency (JAXA). His research interests include antenna for signal processing, radar signal processing of high resolution, radio wave sensor for observation, development of microwave radiometer mounted on space satellite, reconfigurable component, space solar power satellite. He was a guest researcher at the Electroscience Laboratory of Ohio State University from 1997

to 1998.